NPS72-86-001CR

NAVAL POSTGRADUATE SCHOOL

Monterey, California

CONTRACTOR REPORT

A TRANSIENT ONE-DIMENSIONAL MODEL FOR METAL COMBUSTION IN STEAM

Zeev Shavit

August 1986

Approved for public release; distribution unlimited.

Prepared for:

Naval Surface Weapons Center/WOL
Code R10A
Silver Springs, MD 20910

NAVAL POSTGRADUATE SCHOOL
Monterey, California

RADM R. C. Austin
Superintendent

D. A. Schrady
Provost

The work reported herein was carried out for the Naval Postgraduate School by Mr. Zeev Shavit under Contract N62271-85-M-0468. The work presented in this report is in support of "Underwater Shaped Charges" sponsored by the Naval Surface Weapons Center. This work provides a description of a model for metal combustion in steam. The model is built in a general way in which it will be able to adapt to the various phenomena of underwater shaped charge metal burning, exploding wire and transient droplet combustion in rocket motors. The project at the Naval Postgraduate School is under the cognizance of Distinguished Professor Allen E. Fuhs who is principal investigator.

Prepared by:

REPORT DOCUMENTATION PAGE

1a REPORT SECURITY CLASSIFICATION UNCLASSIFIED	1b RESTRICTIVE MARKINGS NONE
2a. SECURITY CLASSIFICATION AUTHORITY	3 DISTRIBUTION / AVAILABILITY OF REPORT Approved for Public Release; Distribution Unlimited
2b DECLASSIFICATION / DOWNGRADING SCHEDULE	
4 PERFORMING ORGANIZATION REPORT NUMBER(S) NPS72-86-001CR	5 MONITORING ORGANIZATION REPORT NUMBER(S) NPS72-86-001CR

6a NAME OF PERFORMING ORGANIZATION Zeev Shavit	6b OFFICE SYMBOL (*If applicable*) 72	7a NAME OF MONITORING ORGANIZATION Naval Postgraduate School
6c. ADDRESS (*City, State, and ZIP Code*) Research Contractor Naval Postgraduate School Monterey, CA 93943-5100		7b. ADDRESS (*City, State, and ZIP Code*) Space Systems Academic Group, Code 72 Monterey, CA 93943-5100
8a. NAME OF FUNDING SPONSORING ORGANIZATION Naval Surface Weapons Center/WOL	8b OFFICE SYMBOL (*If applicable*) NSWC/WOL	9. PROCUREMENT INSTRUMENT IDENTIFICATION NUMBER
8c. ADDRESS (*City, State, and ZIP Code*) Naval Surface Weapons Center White Oak Laboratories Silver Spring, MD 20910		10 SOURCE OF FUNDING NUMBERS

PROGRAM ELEMENT NO	PROJECT NO	TASK NO	WORK UNIT ACCESSION NO

11 TITLE (*Include Security Classification*)

A TRANSIENT ONE-DIMENSIONAL MODEL FOR METAL COMBUSTION IN STEAM

12. PERSONAL AUTHOR(S)
ZEEV SHAVIT

13a. TYPE OF REPORT	13b TIME COVERED	14. DATE OF REPORT (*Year, Month, Day*)	15 PAGE COUNT
Contractor Report	FROM Aug. 85 TO Aug. 86	August 1986	44

16. SUPPLEMENTARY NOTATION

17 COSATI CODES			18 SUBJECT TERMS (*Continue on reverse if necessary and identify by block number*)
FIELD	GROUP	SUB-GROUP	Metal Combustion, Exploding Wire, Transient Droplet Combustion

19 ABSTRACT (*Continue on reverse if necessary and identify by block number*)

The possibility of ignition of some particles of a fragmented Under-Water (U/W) Shaped-Charge (S/C) jet is examined. It was determined that only minute particles (less than 6 micron diameter) are likely to undergo complete melting. This estimate was based on the high stagnation temperature upstream of a particle moving at a speed of 7000 m/sec in water vapor within the cavity.

Some two-color pyrometry tests of exploding wire that had been conducted at the Naval Postgraduate School were re-examined. It is suggested that color photographs of the corona region exhibit on going gas phas combustion. Due to the high temperature (inferred from the color), it is contended droplets do not occur in that region (either metal or oxide). The mode of combustion is distinctly different from metal droplet combustion such as may take place in U/W S/C or in rocket combustion/

20 DISTRIBUTION / AVAILABILITY OF ABSTRACT ☒ UNCLASSIFIED/UNLIMITED ☐ SAME AS RPT ☐ DTIC USERS	21. ABSTRACT SECURITY CLASSIFICATION UNCLASSIFIED
22a NAME OF RESPONSIBLE INDIVIDUAL ALLEN E. FUHS, Chairman	22b TELEPHONE (*Include Area Code*) (408)646-2948 — 22c. OFFICE SYMBOL 72

☆ U.S. Government Printing Office 1986—606-24

19. ABSTRACT

Existing models for metal droplet combustion were found to lack two features, namely full time-dependence and oxide cloud radiation for a large volatile droplet. We suggest to incorporate these features in the proposed model.

For simplicity, only the one dimensional (spherically symmetry) case is considered. Metal liquid to vapor interface is not treated explicitly but through inluding the vapor quality and vaporization latent heat into the total metal enthalpy. The condensed oxide (according to local equilibrium composition), is considered as a second phase. Thus the model ought to be adequate for either volatile or non-volatile process of metal combustion.

ABSTRACT

The possibility of ignition of some particles of a fragmented Under-Water (U/W) Shaped-Charge (S/C) jet is examined. It was determined that only minute particles (less than 6 micron diameter) are likely to undergo complete melting. This estimate was based on the high stagnation temperature upstream of a particle moving at a speed of 7000 m/sec in water vapor within the cavity.

Some two-color pyrometry tests of exploding wire that had been conducted at the Naval Postgraduate School were re-examined. It is suggested that color photographs of the corona region exhibit on going gas phase combustion. Due to the high temperature (inferred from the color), it is contended droplets do not occur in that region (either metal or oxide). This mode of combustion is distinctly different from metal droplet combustion such as may take place in U/W S/C or in rocket combustion.

Existing models for metal droplet combustion were found to lack two features, namely full time-dependence and oxide cloud radiation for a large volatile droplet. We suggest to incorporate these features in the proposed model.

For simplicity, only the one dimensional (spherically symmetry) case is considered. Metal liquid to vapor interface is not treated explicitly but through including the vapor quality and vaporization latent heat into the total metal enthalpy. The condensed oxide (according to local equilibrium composition), is considered as a second phase. Thus the model ought to be adequate for either volatile or non-volatile process of metal combustion.

ACKNOWLEDGEMENT

The author wishes to express his gratitude to Professor Allen Fuhs for providing the opportunity to perform this work during my sabbatical, and for his support in participation as well as for the many valuable discussions.

TABLE OF CONTENTS

LIST OF FIGURES

LIST OF TABLES

NOMENCLATURE

A	constant.
a	velocity of sound.
A_{ci}	internal cloud surface.
A_s	effective contact surface between two phases.
A_w	metal surface area.
B	constant in Eq. 6-34.
c_j	mass fraction concentration of species j.
c_{P_j}	species heat capacity.
c_{P_g}	gas heat capacity.
D_{jk}	binary diffusion coefficient.
D_{j^0}	mixture diffusion coefficient of species j.
E	activation energy.
f	mixture fraction.
F_p	friction force.
h	enthalpy.
H_{fu}	metal heat of combustion.
h_{sf}	solid to fluid latent heat.
h_{fg}	fluid to gas latent heat.
I	radiation intensity.
i	mass stochiometric constant.
k	heat conductivity.
k_{lj}	the k^{th} order coefficient in a polynomial to describe a temperature dependent property of the j^{th} species.
l	effective cloud particle thickness for radiation.
N	number of radiated particles per unit volume.
Nu	Nusselt number.
M	Mach number.
M_j	species molecular weight.
M_{12}	momentum transfer from phase 1 to phase 2.
p	pressure.
Q'''	heat source.
q''	heat flux.
R	specific gas constant.
r	radial distance.
$\mathscr{R}$	phase volume fraction

T	temperature.
s_i	ratio of internal cloud to metal surface area.
s_o	ratio of external cloud to metal surface area.
u	radial velocity.
w''_j	mass source of species j.
α	absorption coefficient.
β	flow parameter in stagnation region.
ε	emissivity.
ϵ	extinction coefficient.
λ	convection heat transfer coefficient.
Ω_{jk}	effective molecular diffusion cross section parameter.
μ	viscosity.
ρ	density.
γ	specific heat ratio.
σ	Boltzmann coefficient.
δ	covered oxide thickness layer.
χ	mole fraction.
Y	stoichiometric mole coefficient.
Θ	nondimensional temperaure.

Subscripts

$_0$	initial.
$_1$	gas and metal phase.
$_2$	oxide phase.
$_c$	convection or cloud.
$_{fg}$	fluid to gas.
$_{fu}$	fuel.
$_g$	gas.
$_H$	hydrogen.
$_m$	melting.
$_M$	metal.
$_{ox}$	oxide.
$_p$	particle.
$_r$	wall radiation.
$_t$	total.
$_s$	solid.
$_{sf}$	solid to fluid.

st	stoichiometric.
wv	water vapor.

Superscript

0	stagnation.

1. INTRODUCTION

Metal particle ignition and burning phenomena have been used for several purposes. In solid rockets metal ingredients enhance the specific impulse and stabilize acoustic waves. In under-water vehicles metal particle burning is used as fuel for its motor. Recently explosive enhancement of Under-Water (U/W) Shaped Charge (S/C) by means of aluminum particle burning in water has been examined, (Ref. 1).

In the case of stand-off explosion of an U/W S/C, a diverging shock wave propagates into the surrounding water. A hypersonic metal particle jet is moving in a radial direction, from the explosive center to the target. As a result of severe heat transfer conditions at the stagnation point ofthe S/C metal jet, some particles may ignite. Ignition will depend on initial particle size, environmental condition and time exposed to heating fluxes. Combustion will enhance the pressure driving the shock wave and tear the target vigorously. Various combustion parameters affect the impulse on the target in an U/W S/C. Some of them are : heat of combustion of metal with steam, initial size of burning particles, flow-field etc.. A close investigation of different type of metals burning in steam was carried out by Exploding Metal Wire (EMW) tests, (Refs. 2-4). The purpose of these tests was to find the best available metal, which due to its burning, will improve the U/W S/C effectiveness. Although, as shown later, there is no similarity in combustion behavior between the U/W S/C and EMW, one can assume that the most effective and energetic metal found in the EMW tests, will also be the best to use in U/W S/C.

Ref. 1 describes some experiments with aluminum shaped charge and a calculation of impulse improving by factor of 1.2 due to complete droplet combustion. Strong transient effects predominate the S/C particles heating process; therefore, ignition and combustion must be carefully examined. In some cases large particles would not ignite, (Ref. 5), and in others existing burning particles may be extinguished. The problem of predicting the amount of metal particle, varied by size, that contributes by combustion to the explosive enhancement, needs to be solved by constructing an appropriate model. Before postulating a new model, we need to understand the various parameters and stages in the general combustion process. We will discuss the metal ignition problem of U/W S/C in water vapor environment. Then we will examine the the governing parameters in the fast combustion process and construct an appropriate model by starting from the differential equations that describe the burning process.

2. GENERAL STAGES IN COMBUSTION

There are three distinct time intervals in the combustion process: ignition, burning and cooling. The ignition stage includes heating of the metal surface to a certain level of temperature where slow chemical reaction will be replaced by near infinite reaction rates. As a result of rising wall temperature, surface reaction rate increases and thus the oxide layer grows. Heat is generated by the reaction, and the progress of the burning process depends on positive supply of heat to the metal. If heat loss rate is larger than the rate of heat released by combustion, the burning will be extinguished. The equation that describes the heat transfer balance is given in Ref. 5 as the following:

$$(1./3.)\rho_{Ms} c_{P_{Ms}} r\partial T/\partial t = \rho_{ox} H_{fu} \partial\delta/\partial t - (k/2r)Nu(T-T_g) \qquad (2\text{-}1)$$

Here δ is the thickness of the oxide layer and can be presented by an Arrhenius type equation. Eq. 2-2 from Ref. 5 describes the kinetic law of oxidation.

$$\partial\delta/\partial t = (B\, c_{ox}^{m}/\delta^{n})\, Exp(-E/(RT)) \qquad (2\text{-}2)$$

Spontaneous high heating rate, like an explosion or fast electrical heating, may cause ignition with a very small growth of oxide layer. Fig. 1 illustrates the difference in temperature rise between the fast and slow heating process. In the spontaneous case, fast heating rate raises temperature high above the ignition point and then, when the combustion is starting, the temperature drops below the level of adiabatic flame temperature. In contrast, combustion due to low heating will occur when the metal surface temperature reaches the ignition temperature.

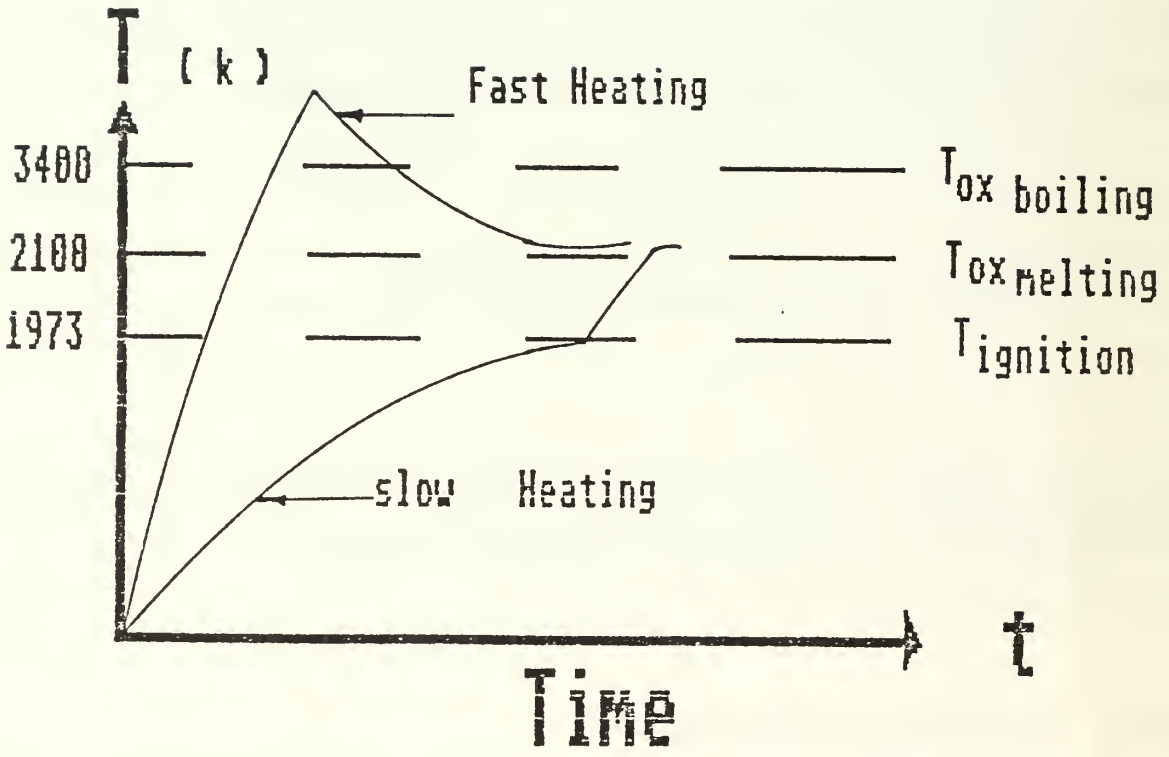

Fig. 1 Temperature rise in fast and low heating rates

Some materials such as aluminum and magnesium have a Metal Boiling Temperature (MBT) lower than its Oxide Boiling Temperature (OBT). In such volatile material, combustion begins just after the metal surface is exposed to the surrounding atmosphere. Exposure of metal surface occur due to surface-tension-induced movement of liquid oxide layer gliding over the liquid metal or by blow-off of the oxide layer as happens in the exploding wire case. Vapor phase reaction will take place in the flame zone as long as heat losses are lower than heat generated by the combustion process. Glassman stated in Ref. 6, that the maximum temperature in the combustion zone is bounded by the oxide evaporation temperature.

Non-volatile metals such zirconium or tantalum has MBT greater than OBT, and since the combustion temperature is lower than OBT, the metal would not be able to evaporate; therefore, combustion will occur on the metal surface, and the oxide product, near the reaction zone, will appear on the gas phase only. Table 1, from Ref. 7, presents some data on MBT and OBT for several useful metals.

Metal	Melting Pt., °C	Boiling Pt., °C	Oxide	Melting Pt., °C	Boiling Pt., °C	Adiabatic Flame Temp., °C (Equilibrium)
Na (Sodium)	97.8	883	Na_2O	---	1770 - 1827	
Mg (Magnesium)	650	1103	MgO	2800	3100	3077
Ca (Calcium)	850	1690	CaO	2590	3500	3527
Al (Aluminum)	660	2500	Al_2O_3	2050	3500	3527
Ti (Titanium)	1730	3260	Ti_2O_3	2100	3000	3027
Zr (Zirconium)	1845	4900	ZrO_2	2690	4300	4527

TABLE 1 Physical properties of some metals and their oxides (Ref. 7)

The composition of the environment has a strong influence on the combustion process. Static pressure as well as oxidizer concentration and type of ingredients determine the rate of combustion. Burning of an aluminum particle in free air is governed by vapor phase

reactions, whereas in rocket motors various species such as CO_2 add some surface reactions to the vapor phase burning droplet (Ref. 8). Volatile metal burning is controlled mainly by vapor phase reactions and produce large quantities of small condensed oxide particles, often called smoke oxide cloud. The small condensed particles (less than 2 micron, Ref. 9) are produced in the flame zone and convected away by the main flow. If the flame zone is close enough to its moving burning droplet, smoke oxide particle may impinge on the metal surface, deposit on it and change its mass and momentum. For large particles the effect of smoke oxide radiation may not be neglected. King, in Ref. 8 neglected radiation effects and therefore limited his solution to a maximum of 30 micron aluminum particle size, and found good results compared with experimental tests in wet oxidizer, Ref. 16. Wood, Ref. 10 observed strong radiation effect on burning magnesium particles greater than 80 micron. Heat flux radiation, emitted from the condensed cloud, cools the reaction zone and heats the evaporating metal surface. A schematic description of the various zones in a burning moving aluminum particle, is given in Fig. 2, taken from Ref. 9.

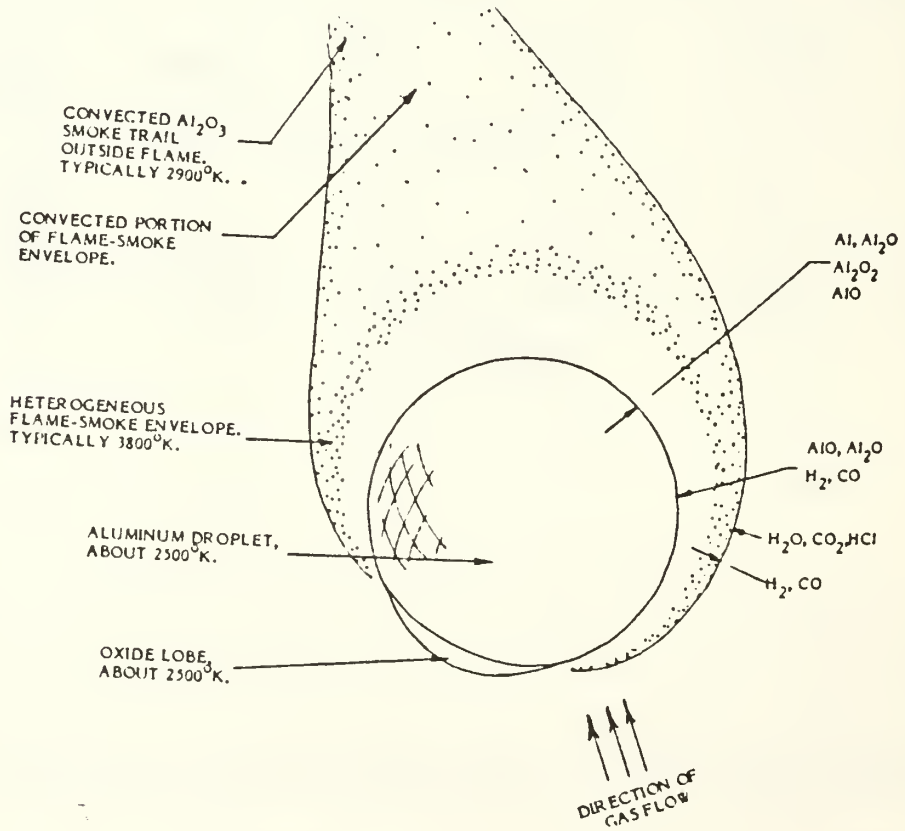

Fig. 2 General nature of the combustion zone of a volatile metal droplet burning in a mild convective flow (Ref. 9)

3. ESTIMATING THE MAXIMUM PARTICLE SIZE FOR IGNITION IN AN U/W S/C

The first step for estimating impulse enhancement of an U/W S/C by means of aluminum combustion is to assure that the moving particles in the S/C jet do ignite under the special conditions.

3.1 Conditions and Method of Estimation

In order to make a quick estimation whether an aluminum particle can reach the burning phase condition, while moving at high speed inside a shaped charge jet of particles cloud at an underwater explosion conditions, we evaluate the time needed by a single particle to increase its temperature to the melting point and become completely molten. If that time, assuming severe conditions, is larger than the transit time from the stand-off explosion to the target then it is impossible for burning conditions.

Time dependent conditions are not taken into account, and a simple calculation is being done by assuming an equilibrium state between water and steam, which means that the cavity is full with saturated steam. These conditions are the most severe boundary condition the shaped charge particles can meet.

Other assumptions made here, are:

- -The surrounding pressure is equal to the hydrostatic water pressure.
- -All particles meet the same conditions and donot exchange heat betwe en themselves.
- -The particle spherical shape does not change.
- -Particle velocity remains constant and equal to 7000 m/sec.
- -Internal temperature distribution is ignored.

3.2 Equations

For the solid state particle the equation of lump heating is:

$$\lambda_c(T_r-T)-\sigma(\varepsilon_w T^4 - \alpha_g T_g^4) = -\rho_{Ms} c_{P_{Ms}} (\partial T/\partial t) \qquad (3\text{-}1)$$

Here λ_c, T_g, T_r and α_g will be calculated according to the steam conditions and the particle velocity. The second equation shows the change in particle radius during melting time

Here λ_c, T_g, T_r and α_g will be calculated according to the steam conditions and the particle velocity. The second equation shows the change in particle radius during melting time

$$\lambda_C(T_r - T_{Mm}) - \sigma(\varepsilon_w T_{Mm}^4 - \alpha_g T_g^4) = -(\rho_{Ms} - \rho_{Mf}) h_{Msf} r_{P_0} \xi^2 \, \partial\xi/\partial t \qquad (3\text{-}2)$$

3.3 Calculation of the Coefficients

a. Saturated Steam Condition at 3 atm.

$T_{wv} = 407$ K ; $\rho_{wv} = 1.68$ kgm/m^3

$R_{wv} = 848/18 = 47.11$ kgf*m/kgm* K

$c_{P_{wv}} / R_{wv} = 4.12\, c_{P_{wv}}$

$\gamma = (1./(1 - c_{P_{wv}} / R_{wv}) = 1.32$

The speed of sound, a:

$a = \sqrt{\gamma R T g_0} = \sqrt{\gamma 1.32*47.11*9.81*407} = 498.38$ m/sec.

Viscosity at T_g: $\mu = 15.*10^{-6}$ kgm/m*sec

Thermal conductivity at T_g: $k = 6.5*10^{-6}$ kcal/m*sec* K

Radiation absorbance, assuming equivalent length of 2 meter and a pressure of 3 atm:

$\alpha_g(3_{atm}*2_m) = 0.7$

b. Recovery Temperature and Stagnation Conditions.

$M = u/a = (7000. / 498.38) = 14.$

$T_r = T(1 + (\gamma\text{-}1)\, rM^2)/2)$

where r is the recovery factor. Assume $r = 0.89$, for turbulent flow.

$T_r = 407.(1 + 0.16*0.89*14^2) = 11766$ K

This is a very high temperature, and we can, therefore, expect dissociation and an improvement in the thermal conductivity and viscosity. The density, viscosity and Prandtl number at the stagnation condition are:

$\rho^0 = (p/ (R_{wv} T_r) = 3. 10^4/(47.11*1176.) = 0.054$ kgm/m^3

$\mu^0 = 40.*10^{-6}$ kgm/m*sec

$Pr^0 = 0.88$

c. Aluminum Properties.

$\rho_{Ms} = 2700$ kgm/m^3

$\rho_{Mf} = 2380$ kgm/m^3

$\rho_{Ms} - \rho_{Mf} = 320$ kgm/m^3

$T_{Mm} = 932$ K

$h_{Msf} = 94.45$ kcal/Kgm

$c_{P_{Ms}} = 0.23$ kcal/kgm* k

$k_S = 0.05$ kcal/m*sec* k

$\varepsilon_W = 0.2$

d. Stagnation Heat Transfer Coefficient.

The heat transfer coefficient is defined as:

$\lambda = \rho_e u_e C_{p_e} St$

St is the Stanton number for stagnation point flow around a sphere

$St = 0.763 (\beta D/u)^{0.5} (Re_D)^{-0.5} (Pr^0)^{-0.6} (\rho^0/\rho)^{0.5} (\mu^0/\mu)^{0.5}$

For Mach number greater than 10, $D\beta/u = 1$.

In order estimate the shortest time for melting, we will assume a small particle diameter of the size of 20 micron, the appropriate Re_D number will then be:

$Re_D = 1.68*7000*20*10^{-6} /15*10^{-6} = 15680.$

The ratio of density at stagnation and free stream and the ratio of viscosities at these two conditions, are:

$\rho^0/\rho = 0.054/1.68 = .032$; $\mu^0/\mu = 40/15 = 2.67$

The heat transfer coefficient is;

$\lambda_c = 1.68*7000*.453*0.763*(15680)^{-(0.5)}*0.88^{-0.6}*(0.32*2.67)^{0.5} = 10.23$ kcal/m^{2}sec K

3.4 Comparison Between Forced Convection and Radiation Heating

The convection term is defined as:

$q_c = \lambda_c(T_r - T)$

Assume particle initial temperature of 500 K

$q_c = 10.23*(11766 - 500.) = 1.153*10^5$ kcal/m^2*sec

Maximum radiation heat losses that can occur at the metal surface are at the highest temperature, $T = T_m$

$q_r = \sigma(\varepsilon_w T_{Mm}^4 - \alpha_g T_g^4) = 1.36*10^{-11}(0.2*932^4 - 0.7*407^4) = 1.46$ kcal/m^2*sec

As q_c is much greater than q_r we may neglect radiation heat losses.

3.5 Diameter Limit for Ignoring Temperature Distribution

Temperature gradient inside matter can be neglected when $k_s/\lambda*r$ is greater than 6. In that case : 0.05/10.23*r is greater than 6. The condition is valid for every particle diameter less than 1630. micron.

3.6 Calculation of Heating Time

The calculation of the heating time needs the solution of the two differential equations (3-1) and (3-2) dropping the radiation term. Without the radiation form the solution is easy at two different periods of time.

a. Conduction in the Solid State Time Interval.

Equation (3-1) can be written for a non-dimensional variable Θ, as follows:

$$(d\Theta/dt) - \tau^{-1}\Theta = 0 \qquad (3\text{-}3)$$

Where: $\Theta = (T_{Mm} - T_i)/(T_r - T_i)$,T_i is the initial temperature, and τ is the time constant and it is equal to : $\rho_{Ms} c_{P_{Ms}} r_{p0}/3*\lambda_c$

The solution for equation (3-3) is:

$\Theta = 1 - \exp(-t/\tau)$

If t_m is defined as the heating time for a particle to reach the nondimensional melting temperature Θ_m, we can find, from the solution of equation (3-3), the ratio of t_m/r_{p0} as a function of the volumeteric heat capacity $\rho_{Ms} c_{P_{Ms}}$ and the heat transfer coefficient λ_c

$$t_m/r_{p0} = -(\rho_{Ms} c_{P_{Ms}}/(3\lambda_c)) [\ln(1 - \Theta_m)] \qquad (3\text{-}4)$$

b. The Melting Time.

Forming the integration Eq.(3-2), by neglecting the radiation term and introducing the boundary condition of $\xi = 1$ when $t = t_m$, yields :

$$\lambda_c(T_r - T_{Mm})(t - t_m) = -(h_{Msf} r_{p0} / 3)(\rho_{Ms} - \rho_{Mf})(\xi^3 - 1) \qquad (3\text{-}5)$$

End of melting occurs when $\Theta = 0$ and at that time $t = t_f$

$$t_f = \tau_m + [h_{Msf} r_{p0} (\rho_{Ms} - \rho_{Mf}) / (3\lambda_c (T_r - T_{Mm})] \qquad (3\text{-}6)$$

Using equation (3-4) for t_m, we will find a general expression for the minimum complete melting time t_f

$$t_f / r_{p0} = (1/3\lambda_c) [- \rho_{Ms} c_{P_{Ms}} \ln(1 - \Theta_m) + (\rho_{Ms} - \rho_{Mf}) h_{Msf} / (T_r - T_{Mm})] \qquad (3\text{-}7)$$

The initial temperature T_i of the particle, at its initial trajectory point, is determined by conservation of energy. We will assume that $T_i = 500$ K, and t_1/r_{p0} will be found by:

$\Theta_m = (932. - 500.) / (11766. - 500.) = 0.0383$

and inserting aluminum metal properties into Eq. (3-7), yields:

$$t_f / r_{p0} = 0.0874 - 20.23 * \ln(1 - \Theta_m) \qquad (3\text{-}8)$$

By introducing $\Theta_m = 0.0383$, into Eq. (3-8) we determine t_f/r_{p_0} equal 66.2 sec/m . Let us assume a traveling time of 200 microseconds for a particle to reach the target. Now we can find, by substituting $t_f = 200$ microseconds, that just 6 micron particles or smaller will completely melt and particles with larger diameter will have no chance to reach the ignition point.

4. EXPERIMENTAL RESULTS IN WATER VAPOR ENVIRONMENT

As mentioned in chapter 2, combustion behaviour varies with the change of the environmental composition. Generally, the burning rate depends on the oxidizer concentration (Refs. 7,16), therefore combustion in water vapor is faster than in air at the same static environmental pressure and temperature. On the other hand, ignition in water vapor is more difficult than in air. The oxide layer deposit in wet environments is more protective than in dry environments and therefore ignition temperature in water vapor is 1700 K (Ref. 8), whereas in dry air, about 1000 K. The predominant reaction of aluminum in water has the form of:

$$2\,Al + 3\,H_2O = Al_2O_3 + 3\,H_2$$

Wilson et al. (Ref. 11) found the reaction rate constants for the above reaction.

$$K = 4.916\ 10^{8}\ Exp[\ -73.5/(1.99T)] \qquad (4\text{-}1)$$

Ref. 11 also mentioned that the condensed oxide smoke is carried away faster in moist steam than in dry air. Ref. 7 found that hydrogen attacks the oxide deposition layer causing porosity and, therefore, greater vapor metal fuel consumption.

Experiments with exploding wire in steam were carried out by Kol et al., Refs. 2-4. Fig. 3, from Ref. 4, shows an example of magnesium exploding wire and its different main combustion regions. The white brightest sphere at the center is the plasma core. Its temperatures high above 6000 K, and it contains partially ionized metal vapor. The outer spherical shell consists of metal vapor, where a temperature higher than the OBT is maintained. On the outer surface, the metal vapors meet the surrounding steam, and vapor phase reactions occur.

Since radiative and conductive heat fluxes from the plasma core to the metal vapor shell are high, metal vapor temperature is expected to be much higher than the OBT. Because of

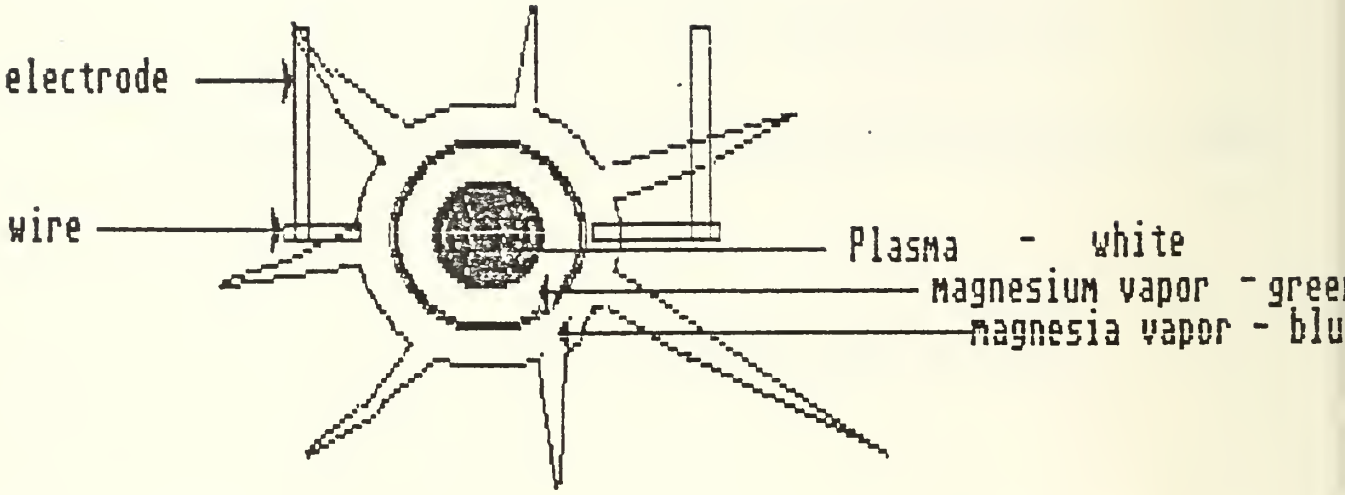

Fig. 3 Magnesium exploding wire - region of combustion in steam
(from Ref. 4)

these enormous heat fluxes and high temperatures, the system can not be considered as an adiabatic system, and, hence, local oxide product may still appear on the gas phase. Results of measurements presented in Ref. 4 show that up to a Normalized Distance (ND) of 120 from the plasma core center, the cloud and its streaks are blue and the temperature is above the OBT. Beyond this distance, color is changing and temperatures, detected by a two color photo-pyrometry technique, indicate condensation of the oxide gas species. Overall maximum resolution of the measurement device is 2 micron, and, therefore, it could not resolve the small condensed oxide particles in the streak. As a consequence of the above measurement results, the author concludes that the cloud around the exploding

wire consists of plasma, gas phase reactant and gas products. Due to high temperatures in that region, metal vapor and oxide product condensation is not possible in the corona sphere close to the exploding center. Oxide product condensation may take place just after expanding away from the explosion center. As a result of the wire explosion, some of its molten parts are blowing-off as metal droplets and appear beyond the corona's streaks. Fig. 4, which presents a schematic model for emission from the metal droplet, is based on a color slide picture taken in a magnesium wire explosion test. In some cases, one can assume that hot droplets emitted from the hottest melted wire may ignite, but most of them do not. They simply cool and condense along their trajectory in steam. Ref. 2 describes measurement results of the high particle deceleration (of the order of 100000. m/s^2), caused by growth of liquid alumina on the surface of moving burning metal droplets. In most deceleration measurements, in Ref. 2, the solid oxide particles were the product of abrupt solidification of molten super cooled droplets.

The various cases, described above, present the complexity of the phenomena of metal combustion under various environmental and initial conditions. In order to have better estimates, there is a need for a calculating tool. The next chapter is devoted to describing the transient combustion.

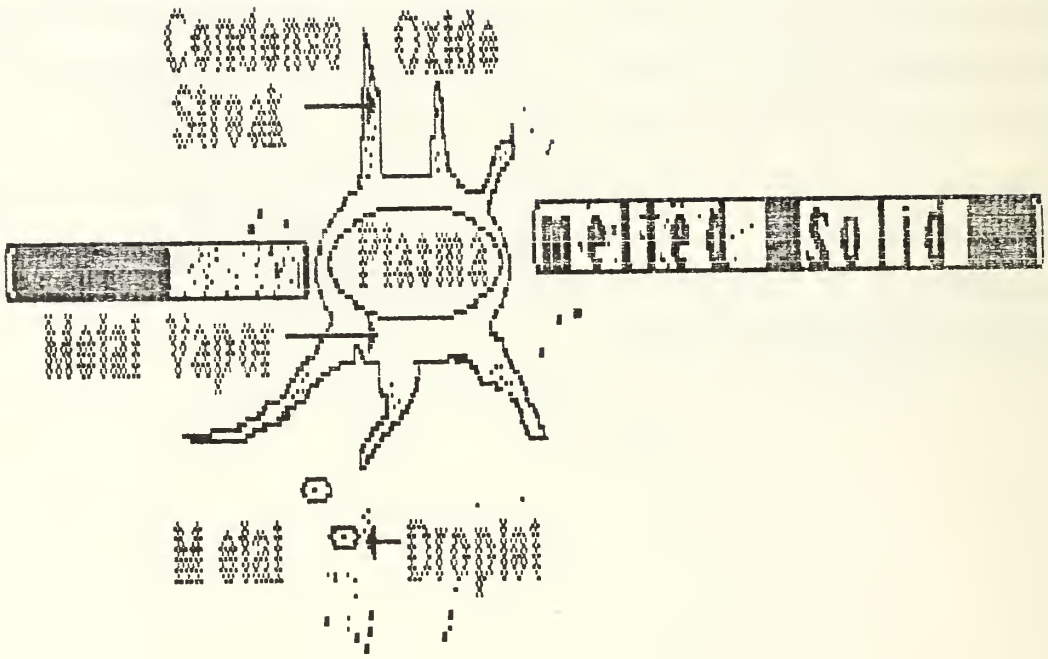

Fig. 4 Regions surrounding a metal exploding wire

5. DISCUSSION OF PARAMETERS FOR MODELING THE METAL COMBUSTION

Exploding wire and underwater shaped charge metal jet are just two instances of a very fast, non-steady phenomena. Even metal particles ignition and combustion in a rocket motor environment cannot always be considered as a quasi-steady process. A precise prediction of ignition time, temperatures and species existing in the various combustion regions can be done only if transient effects are included.

All quasi-steady combustion models (Refs. 6,8,12) assume Lewis Number unity, which physically means that the evaporating metal mass flux is independent of the gas phase reaction rate. That assumption may not be valid in any of the following circumstances: Reactions are kinetically controlled , strong mass convection effect and dissociation caused by high temperature. Those chemical and flow conditions may certainly be present at the beginning and the end of the combustion process of a moving metal droplet.

The fact that the moving burning metal droplet accumulates part of its oxide product induces a dramatic changes in its velocity, Ref. 2. A physical model will be required to describe the evolution in time of the various parameters. In order to achieve that model, solution of the flow field, mass and heat transfer equations is needed. It is also important to estimate the radiation and the effect of deposition of smoke oxide cloud particles on the burning metal droplet. It is necessary to account for the flow as two-phase flow together with radiation terms. Radiation fluxes from the condensed oxide causes heat losses from the reaction zone and heats the burning surface. As a consequence of two-phase flow heat and momentum are delivered from one phase to the other, and convection terms between two phases change temperatures and velocities. Therefore, these effects should not be ignored.

For the same kind of metal and environmental conditions, differences in results between the various 1-D, quasi-steady models (Refs. 6,8,12) and unsteady, 2-D two-phase flow model are expected. The validity of including the volatile and non-volatile metals in one model has not yet been demonstrated. The idea of joining them into one model is based under the following thermodynamic facts. The difference between these two types of metal is mainly in the reaction zone location and behavior of oxide product. By solving the coupled conservation equations, one can find the distribution of enthalpy and vapor concentration distribution in time and space. But metal surface temperature and location are yet not known. By writing the mixture total enthalpy expression and including terms of species concentration, heat of formation, metal phase-change enthalpy, and by employing the parameter of vapor metal quality and the thermodynamic relationship of wall temperature and metal-vapor concentration, one can eliminate the instantaneous surface location and its temperature. In the case of non-volatile metal combustion, the thermodynamic dependence of surface metal temperature on vapor concentration along with solution of conservation equations will result in the highest temperature being on the burning metal surface. Whereas in the case of volatile metal burning, the point of highest temperature may be anywhere in the field. Oxide condensation takes place whenever the local gas temperature is lower than OBT. Since MBT of a non-volatile metal is greater than OBT,

oxide condensation may appear at a large stand off from the metal surface. In contrast, for volatile metal, condensation of oxide may be on the metal surface. The above discussion shows that by applying the thermodynamic phenomena description and the conservation equation, a general transient model can be formulated for volatile as well as for non-volatile metal combustion. The next step will describe the governing equations of such a model.

6. GOVERNING EQUATIONS

The various cases of exploding wire or droplet metal combustion in steam can be solved by one general model, which includes the transient, two-dimensional, asymmetrical effects. For the sake of simplicity, since we are interested in investigating the transient two phase flow and radiation effects, we will first consider the problem in transient one-dimensional, spherical configuration.

6.1 Energy Equation for Gas and Liquid Metal

The equation will be written for enthalpy and will include in one region (subscript 1) the various gas species and liquid metal as well. Properties at each point will be presented as dependent on species mass fraction and local temperature. Assuming constant static pressure in the entire region, the equation in the radial direction will be given as follows:

$$\partial(\rho_1 h_1)/\partial t = r^{-2}\partial[r^2 K_1(\partial T_1/\partial r)]/\partial t + Q''_1 - \rho_1 u_1 \partial(h_1/\partial r) \qquad (6\text{-}1)$$

Where the mixture enthalpy is given by:

$$h_1 = \Sigma h_i c_i \qquad (6\text{-}2)$$

c_i is the mass fraction of species i, and h_i is given by:

$$h_i = h^0_i + \int c_{p_i} dT \qquad @\ i = \text{Metal}, H_2O, H_2 \qquad (6\text{-}3)$$

Metal enthalpy, h_M , will account for quality of metal vapor, x, and phase change enthalpy, h_{Mfg}

$$h_M = h_{Mg} + (1 - x)h_{Mfg} \tag{6-4}$$

The heat source, Q''_1, is the sum of other various sources, Q''_{1_i} :

a. Heat released by metal combustion :

$$Q''_{11} = w''_M H_{fu} \tag{6-5}$$

b. Heat released by condensation and/or solidification of oxide product :

$$Q''_{12} = w''_{ox} h_{oxfg} \quad @\ T = T_{oxb} \tag{6-6a}$$

$$Q''_{13} = w''_{ox} h_{oxfs} \quad @\ T = T_{oxm} \tag{6-6b}$$

Two assumptions are made here. The first is based on the idea that oxide phase change will occur if local temperature is lower then the OBT or lower then Oxide Melting Temperature (OMT). The other assumption is based on the fact that mass transfer between phases is a comparatively fast process.

c. Heat transfer from one phase to the other.

$$Q''_{15} = (h_c A_s / V)(T_1 - T_2) \qquad (6\text{-}7)$$

d. Radiation heat source due to cloud particles.

q''_{r_c} and q''_{r_w} are the heat radiation sources, located at the cloud and at the wall respectively. Later-on, we will develop those two radiation terms. In general, q''_r stands for radiation flux, and and the radiation source will be:

$$Q''_{14} = q''_r / l \qquad (6\text{-}8)$$

The solution of the energy equation together with the conservation equations will produce an enthalpy distribution for each time step. Temperature and metal metal vapor distributions can be eliminated from these transport equation results. Going from the far outer gas edge toward the metal surface, whose location has yet not been determined, the following sequencing logic should be adopted. For each nodal point, we need to determine whether liquid metal existed there at the previous time step. It is assumed that once the gas phase appears it will remain gas and liquid metal cannot appear again at that nodal point. If gas phase existed, x will be remain equal to unity, and the temperature will be computed from the calculated local enthalpy and gas species mass fraction. This assumption is justified by the fact that in most combustion stages, metal vapor is totally consumed in the reaction zone, and its concentration during the ignition period is very small.

By assuming a constant value of C_p, enthalpy for each species can be defined as follows :

For fully melted metal ingredient at T_{Mm} temperature.

$$h_{M1} = c_{P_{Ms}} (T_{Mm} - 298.) + h_{Msf} \quad (6\text{-}9)$$

For fully vaporized metal ingredient at T_{Mb}.

$$h_{M3} = h_{M1} + c_{P_{Mf}} (T_{Mb} - T_{Mm}) + h_{Mfg} \quad (6\text{-}10)$$

Enthalpy of vapor metal ingredient when T is greater than T_{Mb} is given by:

$$h_{Mg} = h_{M3} + c_{P_{Mg}} (T - T_{Mb}) \quad (6\text{-}11)$$

Enthalpy of steam ingredient at the saturation temperature will include its heat of formation, h_{wv}^{0}, at 298. K and phase change latent heat, h_{wfg}.

$$h_{wsv} = h_{w}^{0} + C_{P_{wf}} (T_{wb} - 298.) + h_{wfg} \quad (6\text{-}12)$$

Water vapor ingredient enthalpy at temperature above the saturation point will include h_{wsv}.

$$h_{wv} = h_{wsv} + c_{p_{wv}} (T - T_{wb}) \qquad (6\text{-}13)$$

Hydrogen product of combustion will always appear in the gas phase, and its enthalpy term will be :

$$h_H = c_{p_H} (T - 298.) \qquad (6\text{-}14)$$

According to Eq. 6-2 the total enthalpy of the gaseous mixture is defined as :

$$h = h_M c_M + h_{wv} c_{wv} + h_H c_H \qquad (6\text{-}15)$$

After introducing the terms for each ingredient enthalpy Eqs. 6-11,13,14 and defining C_{P_g} as :

$$C_{P_g} = c_{pMg} c_M + c_{p_{wv}} c_{wv} + c_{p_H} c_H \qquad (6\text{-}16)$$

The temperature at the nodal gas phase can be eliminated, and its expression is :

$$T = [h - (h_{M3} - c_{p_{Mg}} T_{Mb}) c_M - (h_{wsv} - c_{p_{wv}} 373.) c_{wv} - c_{p_H} c_H 298.] / (C_{P_g}) \qquad (6\text{-}17)$$

If at the previous time step, x was less than 1, or even equal to 0., the procedure for determining a new value for x, should be as follows :

By knowing the local metal vapor mass fraction and the total local molecular weight, assume the local temperature to be equal to T_{Mb}

$$T_{Mb} = A / [B - \ell n((c_M M_t) / M_M)] \qquad (6\text{-}18)$$

For aluminum A = 36560.8 and B = 25.016.

Metal vapor quality value, x, can be eliminated from the total enthalpy expression. By assuming that the nodal ingredient mixture consists of saturated metal vapor, water vapor and hydrogen, and assign the local temperature equal to $T_{Mb,}$ x remains the only unknown and, therefore, can be eliminated:

$$x = [h - (h_{M1} + c_{P_{Mf}}(T_{Mb} - T_{Mm})c_M - (h_{wsv} + c_{P_{wv}}(T_{Mb} - 373.))c_{wv} - c_{P_H}(T_{Mb} - 298)c_H]/ (h_{Mfg}c_M) \qquad (6\text{-}19)$$

If the resulting value of x, based on those assumptions, is larger than one, then the local temperature should be greater than the assumed temperature T_{Mb}, and a new tentative value of temperature should be determined by using Eq. 6-17. If , at the first iteration x becomes equal to or greater then zero, then the temperature is set equal to T_{Mb} and the surface location is determined. Further inside the metal, temperatures are determining by setting x equal to zero.

$$T = (h - h_{M1} + c_{P_{Mf}} T_{Mm}) / c_{P_{Mf}} \qquad (6\text{-}20)$$

The thermodynamic relationship for the metal vapor density shows that increasing of x will decrease the density ρ_M, Eq. 6-21. Metal surface vaporization cause a local density decrease and since the continuity law must also be conserved, the net metal vapor will expand outward to the gas surrounding.

$$\rho_M = \rho_{Mg} / [1 + (1 - x)(\rho_{Mg}/\rho_{Mf} - 1)] \qquad (6\text{-}21)$$

6.2 Determining the Effective Radiation Heat Source

Considerable amounts of radiating heat fluxes govern the metal combustion process in the case of large volatile particles. In most other cases the surrounding gas can be considered as an optically thin medium. When oxide particles appear, the media is not transparent any more. The number of particles per unit volume N, the particle size r_p, specific particle emissivity, cloud thickness l, and the relative geometric location of the particle cloud determines the radiation fluxes.

Intensity attenuation of radiation propagating through a particle cloud is given in Ref. 13 as:

$$I/I_0 = EXP(-\epsilon l) \qquad (6\text{-}22)$$

Where the extinction coefficient ϵ is a function of N and r_p. Measurement results described in Ref. 13 demonstrate the validitiy of the relationship between these parameters. We present in Fig. 5 some data results of aluminum oxide cloud, which will be used as a data base for our model.

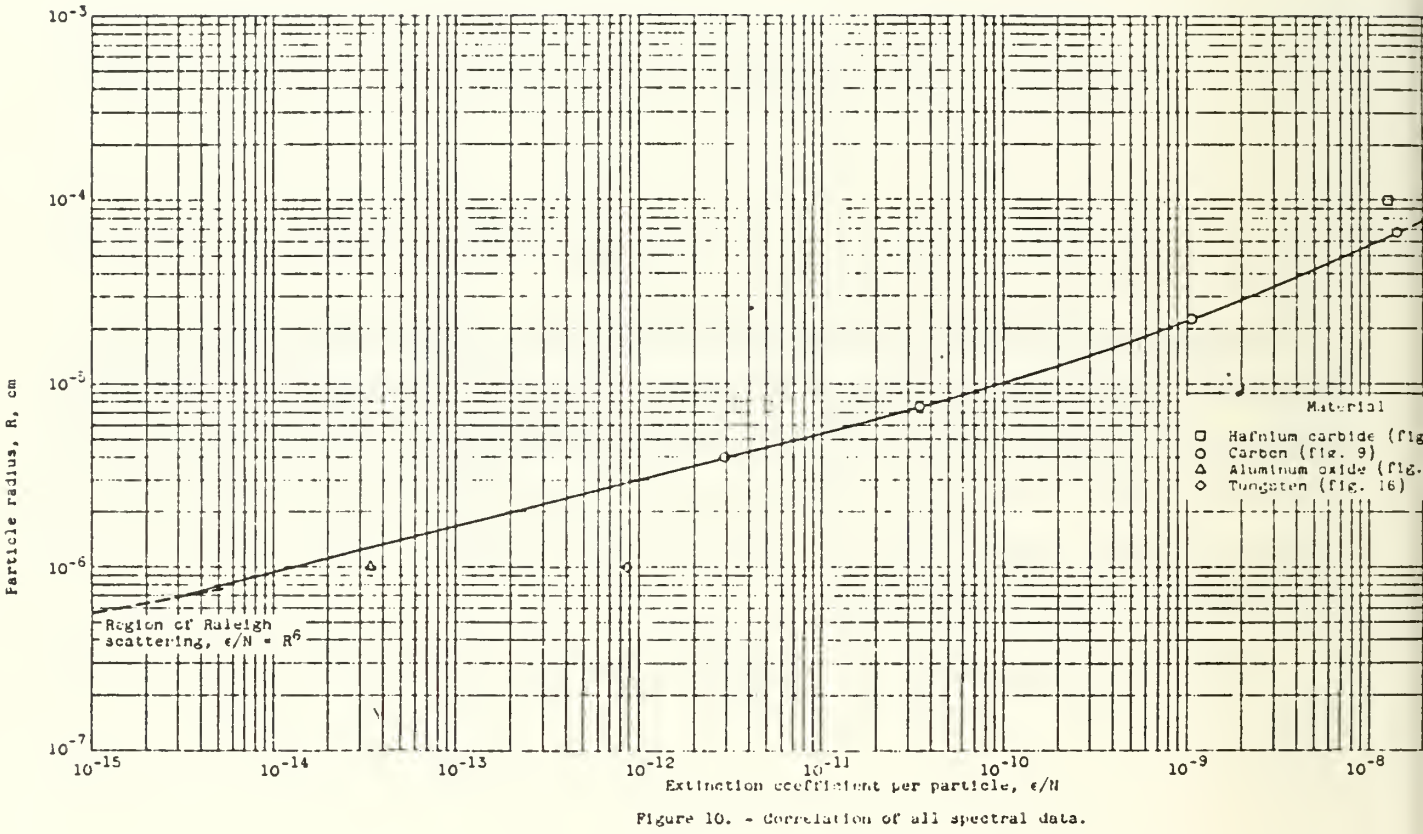

Figure 10. - Correlation of all spectral data.

Fig. 5 Correlation of all spectal data. (from Ref. 13)

Solution of the gas phase chemical reaction along with the other conservation equations will produce the oxide product distribution in the field. By assuming an average particle size r_p, and knowing the local cell density, we are able to determine the number of local oxide particles in that particular volume cell :

$$N_i = (3./4.\pi r_p^3)\,(\rho_i/\rho_{ox}) = \mathscr{R}_2 V/(4\pi r_p \&S''^3./3) \qquad (6\text{-}23)$$

By accounting for all nodal N_i's and their radial position, it is simple to find the total particles cloud depth and its average number of particle per unit volume.

$$N = (\Sigma N_i \Delta V_i) / (\Sigma \Delta V_i) \qquad (6\text{-}24)$$

Using the chart in Fig. 5, we can find the value of ϵ then the overall cloud emissivity ε_p, is determined from :

$$\varepsilon_p = 1 - EXP (- \epsilon l) \qquad (6\text{-}25)$$

Fig. 6 shows directions and radiation fluxes interchanges between the cloud, the metal surface and the environmental gas. For practical purposes it is assumed that all media involved are grey. As the gas is optically thin, and particles are mainly concentrated in a narrow zone (usually the flame zone), isothermal radiating surfaces is a resonable assumption. Total particle cloud radiation is diffused toward the metal surface and to the outer gas space. Part of the radiation emitted from the cloud and impiging on the metal surface, will be reflected back to the cloud by the grey metal wall and absorbed either by the particles in the cioud or by the gas. The net result of radiation fluxes through the particles cloud is also a function of the mean gas and particle cloud temperatures, T_g, T_{ox} and wall metal temperature T_w

$$(q''_{ox_{net}}/\sigma) = \alpha_p \varepsilon_w T_w^4 F_{w-c} s_i + \alpha_p \varepsilon_g T_g^4 s_o + \alpha_p (\varepsilon_p T_{ox}^4 (1-\alpha_w) F_{w-c} s_i - \varepsilon_p T_{ox}^4 \qquad (6\text{-}26)$$

The s_i and s_o are parameters of surface ratios, as shown in Fig. 7 and for spherical geometry they are given by :

$$s_i = A_{ci} / (A_{ci} + A_{co}) = r_{ci}^2 / (r_{ci}^2 + r_{co}^2) \qquad (6\text{-}27)$$

$$s_o = A_{co} / (A_{ci} + A_{co}) = r_{co}^2/(r_{ci}^2 + r_{co}^2) \quad (6\text{-}28)$$

The geometrical view factor F_{c-w} is given as:

$$F_{c-w} = [1./ (\varepsilon_w^{-1} + (\varepsilon_p^{-1} - 1)(A_w/ A_{ci}))] \quad (6\text{-}29)$$

The metal surface absorbs radiation from the particle cloud and the gas while emitting its radiation heat flux outward.

$$(q_{w_{net}}''/\sigma) = \alpha_w \varepsilon_p T_{ox}^4 F_{c-w} + \alpha_w \varepsilon_g T_g^4 - \varepsilon_w T_w^4 \quad (6\text{-}30)$$

Those two radiating fluxes divided by the appropriate characteristic length, which is the particle cloud thickness, provide the local corresponding heat source that should be taken into account as source terms in the energy equation.

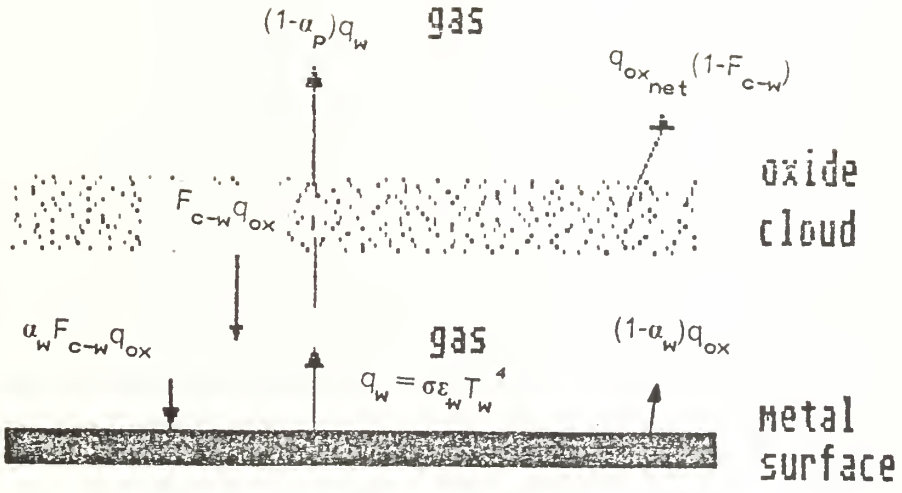

Fig. 6 Radiation heat fluxes exchange between the oxide cloud and the metal surface.

6.3 Energy Equation for the Oxide Particle Phase

The smoke oxide product of a volatile metal combustion requires an energy equation, as it is a second phase in the field. Since the small oxide particles are dispersed in the gas, conduction heat exchange between them can be neglected. The heat transfer time constant for the largest oxide particle (which is less than 2 micron), in a laminar flow is less than 10 microseconds, therefore the radiation heat losses of the particle cloud may be incorporated as a source term in the gas phase energy equation. If local temperature is smaller than the OBT, then immediate condensation of all the new amount of the oxide product will occur.

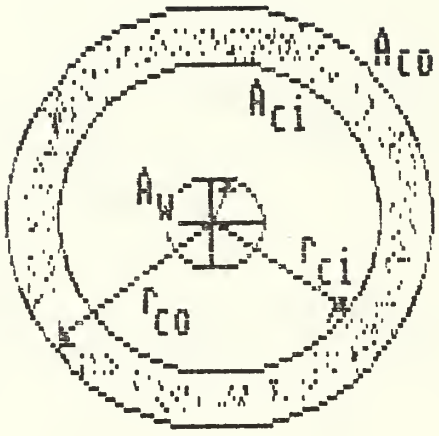

Fig. 7 Geometrical relationship between the cloud and metal droplet.

If $\mathscr{R}_2$ represents the volume fraction of phase 2, then the contact surface A_s, between the oxide particles with an average radius r_p in a volume V is given by Ref. 14 as:

$$A_s = 3\mathscr{R}_2 V / r_p \qquad (6\text{-}31)$$

The source term for that phase will include internal-phase heat transfer and release of latent heat. Ref. 14 presents the source term as :

$$Q_2'' = \lambda_c(A_s/V)(T_2 - T_1) - w_{ox}'' h_{oxfg} \qquad (6\text{-}32)$$

The energy equation will, therefore, be presented as :

$$\partial(\rho_2 h_2)/\partial t = Q_2'' - \rho_2 u_2 \partial h_2/\partial r \qquad (6\text{-}33)$$

The oxide temperature can be directly found from its enthalpy h_2

$$T_{ox} = (h_2 - h_{ox}^0 - c_{P_{ox}} 298.) / c_{P_{ox}} \qquad (6\text{-}33a)$$

6.4 Mass Transfer Equation for Each Species

Analytical descriptions of species mass fraction and enthalpy transport are of the same kind as the general diffusion equation. At some time, when Lewis Number equals 1., their non-dimensional solutions are the same. The distribution in time and space of both variables, c_i and h, are given by the solution of a diffusion equation. With the assumptions of quasi-steady combustion and unit Lewis Number unity, the numerical problem reduces to an algebraic set of 9 equations, (Ref. 8). But in many particular combustion cases, such as an exploding wire or a composite propellant, high temperatures cause dissociation, so that assumption is not valid any more. Simultaneous solution of the diffusion equation is needed with careful attention to various source terms and temperature dependence of the species properties. The source term in the mass transfer equation is the mass production

or consumption of the each particular species. At each time step and location, the source term is determined by local thermodynamic condition. If the local temperature is not high, enough the species source term will be determined by the reaction rate as:

$$w_M'' = B\, T^n EXP(-E_M/RT) C_M^{\upsilon}{}_M C_{wv}^{\upsilon}{}_{wv} \qquad (6\text{-}34)$$

If the reaction rate consumes more than the species mass flux into the local volume cell, then the local consumption and production are controlled by the 'fuel' and 'oxidizer' diffusion rates. If the local mixture ratio f, Eg. 6-35a is less than the stochiometric mixture ratio f_{st} (Eq. 35b), then the new value of the local oxidizer, (water vapor), mass fraction, will be governed by the mixture fraction and all the fuel, (metal vapor), will be consumed. A new value for fuel mass fraction will be set and complete consumption of the oxidizer will occur when f is greater than f_{st}. This procedure is presented graphically in Fig. 8, and Eqs. 36 show its analytical representation.

$$f = 1./(1 + c_{wv}/c_M) \qquad (6\text{-}35a)$$

$$f_{st} = 1. / (1. + (c_{wv}/c_M)_{st}) \qquad (6\text{-}35b)$$

For $0 < f \leq f_{st}$ $\quad c_M = 0$ (6-36a)

For $1 \quad f \geq f_{st}$ $\quad c_{wv} = 1. - f/f_{st}$, $\quad c_{wv} = 0.$, $\quad c_M = (f - f_{st})/(1 - f_{st})$ (6-36b)

The products mass fractions are determined according to the stochiometric ratios i. One Kgm of aluminum will produce $i_{ox} = 1.88653$ kgm of alumina and $i_H = 0.11898$ kgm of hydrogen, in the process it will consume $i_{wv} = 0.998$ kgm of water. The net rate of oxide production will depend on the mixture condition and mass fraction of the reactants.

For a fuel rich mixture the oxide mass fraction source is:

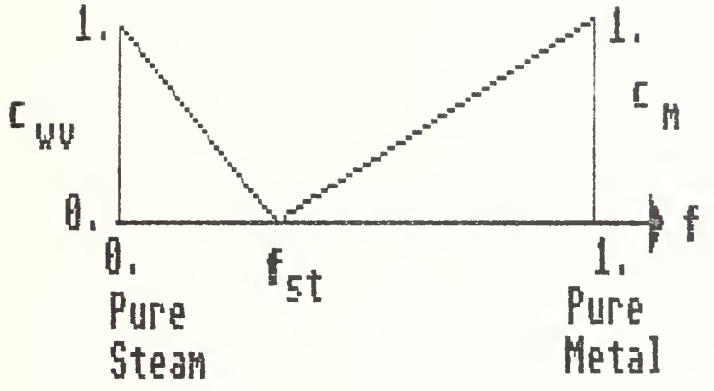

Fig. 8 Mass fraction distribution with mixture fraction.

$$w_{ox}'' = (i_{ox} / i_{wv})\partial(c_M \rho_1 \mathscr{R}_1)/\partial t \qquad (6\text{-}37a)$$

and, for the fuel lean case, it is:

$$w_{ox}'' = i_{ox}\partial(c_M \rho_1 \mathscr{R}_1)/\partial t \qquad (6\text{-}37b)$$

Since the hydrogen product will always appear in the gas phase, we are allowed to set its mass fraction equal to:

$$c_H = 1-c_M-c_{wv} \tag{6-38}$$

The diffusion equation for the mass transport of species j is given by;

$$\partial(\rho_1 c_j)/\partial t = r^{-2}\partial[r^2 \rho_1 D_{jo}(\partial c_j/\partial r)]/\partial r + w_j''' - \rho_1 u_1(\partial c_j/\partial r) \tag{6-39}$$

The density is the density of the local mixture, and D_{i0} is the species diffusion to the mixture. Late in chapter 6.7, we will show how to specify the local properties.

6.5 The momentum equations for each phase

The two phases have the same type of the momentum equation with a source term that stands for the momentum exchange between them. We assume the second phase consists of solely oxide particles. Since the particles are dispersed in the gas, they do not exert friction forces on each other, and, therefore, we may ignore the momentum transport within that phase. We now define the source term of momentum interphase transfer. From Stock's flow around one particle we know that the friction force,F_p ,is given by :

$$F_p = 6\pi\mu r_p(u_1 - u_2) \tag{6-40}$$

Now we define F_p''' as the force F_p per unit

particle volume.

$$F_p'' \equiv F_p/(4\pi r_p^3/3) = 4.5\,\mu/r_p^2 \qquad (6\text{-}41)$$

If $\mathscr{R}_1$ and $\mathscr{R}_2$ are the volume fractions of phase 1 and 2 respectively, then the momentum interphase exchange per unit volume and time will be presented as follows:

$$M_{12} = -M_{21} = F_p''\mathscr{R}_1\mathscr{R}_2\,V(u_1 - u_2) \qquad (6\text{-}42)$$

The radial one-dimensional momentum equation for each phase will then be given by:

$$\rho_1(\partial u_1/\partial t) = r^{-2}\partial\,[r^2\rho_1\mu_1(\partial u_1/\partial r)]/\partial r - \rho_1 u_1(\partial u_1/\partial r) + M_{21} \qquad (6\text{-}43)$$

$$\rho_2(\partial u_2/\partial t) = -\rho_2 u_2(\partial u_2/\partial r) + M_{12} \qquad (6\text{-}44)$$

Since we solve the gas and the metal as one phase by ignoring surface tension forces between them, the metal droplet may be smeared into the gas. In order to prevent that, both phase velocities inside the metal should be set equal to zero. For small enough time step the procedure of freezing velocities will capture the oxide on the metal surface, and therefore simulate deposition.

The total diffusion of species j into a mixture which contains a mole fraction χ of that species, is defined by D_{j0}:

$$D_{j0} = (1 - \chi_j) / (\Sigma(\chi_k / D_{jk})) \qquad (6\text{-}49)$$

The mole fraction χ_j, can be found from c_j , M_t and M_j as follows:

$$\chi_j = c_j M_t / M_j \qquad (6\text{-}50)$$

The mixture conductivity and viscosity coefficients can be found from gas tables Ref.15. They are expressed as a fourth degree temperature polynomial for each species present in the mixture. The conductivity k_j , the viscosity μ_j and heat capacity c_{P_j} will be presented as:

$$k_j = \Sigma k_{1j} T^1 \qquad (6\text{-}51a)$$

$$\mu_j = \Sigma \mu_{1j} T^1 \qquad (6\text{-}51b)$$

$$c_{P_j} = \Sigma c_{P_{1j}} T^1 \qquad (6\text{-}51c)$$

In order to evaluate the mixture viscosity, a bi-molecular viscosity parameter Ω_{jk} should be defined :

$$\Omega_{jk} = (1./\sqrt{8})(1 + M_j/M_k)^{-1/2}[1 + (\mu_j / \mu_k)^{1/2}(M_k/M_j)^{1/4}]^2 \qquad (6\text{-}52)$$

μ is defined as:

$$\mu = \sum [\chi_j\mu_j / (\Sigma(\chi_k\Omega_{jk}))] \qquad (6\text{-}53)$$

The mixture conductivity will be written as:

$$K = \sum [\chi_j k_j / (\Sigma(\chi_k\Omega_{jk}))] \qquad (6\text{-}54)$$

The density ρ_1 is defined by the ideal gas equation of state.

$$\rho_1 = p/(RT_1) \qquad (6\text{-}55)$$

$c_{P_{Mg}}$ was defined previously, in 6-1 when discussed the gas energy equation. The next step should be to cast the model, presented above, in the form of a computer program.

7. SUMMARY

Preliminary calculation for aluminum particles from a shaped charge revealed that the maximum size of a particle that may reach ignition conditions while moving at speed of 7000. m/s during 200 microseconds in a steam environment, is just 6 micron.

Exploding wire experiments in water vapor chamber is an adequate technique for finding the most combustion effective metal liner of underwater shaped charge. However, it does not simulate the phenomena of ignition and combustion of high speed moving metal particles in the U/W S/C. The need for precise prediction in any of these cases requires a solution, which will account for the transient effects along with two phase flow and radiation fluxes emitted from the oxide cloud. The combustion process parameters that will generalize the model for both the volatile and non-volatile metals cases are: the metal vapor quality, surface temperature and metal vapor surface concentration. By writing the energy equation for total enthalpy that include those parameters and accounting for local metal and oxide phase change temperatures, the solution will be valid for both type of metals. The conservation equations were written for the entire region, gas and liquid. The technique of iterating in order to find the metal surface was described. Radiation is accounted for as source terms in the oxide and at the metal surface.

Such a solution for a general type of metal burning will simplify the computer code program for the various cases.

REFERENCES

1. Fuhs A., Buck J. and Strott J., "Metal Combustion in Steam," AIAA paper 84-0204, Jan. 1984.
2. Kol J., Fuhs A. E. and Berger M., "Experimental Investigation of Aluminum Combustion in Steam," Twenty Third AIAA Aerospace Science Meeting, AIAA-85-0323, Jan. 1985.
3. Kol J., Fuhs A. E. and Chozev Y., "Burning Time and Size of Aluminum, Magnesium, Zirconium, Tantalum, and Pyrofuze Particles Burning in Steam," 4th Thermophysics and Heat Transfer Conference, AIAA 86-1336, June 1986.
4. Kol J., Fuhs A. E. and Chozev Y., "Experimental Investigation of Magnesium Combustion in Steam," Twenty Second Joint Propulsion Conference, AIAA-86-1497, June 1986.
5. Frolov Y. V, Pokhil P. F. and Logachev V. S., "Ignition and Combustion of Powdered Aluminum in High-Temperature gaseous Media and in a Composition of Heterogenous Condensed Systems", Fizika Gorenia i Vzryva, Vol. 8, No. 2 pp. 213-236, April-June, 1972.
6. Brzustowski, T. A. and Glassman I., "Vapor-Phase Diffusion Flames in The Combustion of Magensium and Aluminum", Progress in Astronautics and Aeronautics, Vol. 15, 1964, Academic Press, NY and London, pp. 117-158.
7. Long H. C. and Sebald H., "The Burning Rate of Aluminum and Magnesium Wire in Pure Oxygen-Water Vapor Atmospheres at Higher Pressures," Western States Combustion Institute- 68- 8, April 1968.
8. King M. K., "Modeling of Single Particle Aluminum Combustion," AFOSR Report No. AFOSR-TR-78-0060, Nov., 1977.
9. Price E. W., "Combustion of Metalized Propellants," Fundamentals of Solid-Propellant Combustion. Progress in Astronautics and Aeronautics Vol. 90, 1984.
10. Wood W. A., "Metal Combustion in Deflagrating Propellant," ARS Progress in Astronautics and Rocketry: Solid Propellant Academic Press, New-York, 1960, Vol. I, pp. 271-278.
11. Wilson R. E., Mishler L. and Barnes C., "Studies of the Aluminum-Water Reaction by the Levitation Melting Method," ANL - 6648, Chemical Engineering Division Summary Report,

Oct. - Dec., 1962.

12. Law C. K., "A Simplified Theoretical Model for the Vapor Phase Combustion of Metal Paticle," Combustion Sience and Technology, Vol. 7, pp 197-212, 1973.
13. Chester D. and Ragsdale G. R., "Experimental Determination of Spectral and Total Transmissivities of Cloud of Small Particles," NASA TN D-1405, Sept. 1962.
14. Maratos N. C., "Computation of Multi-Dimensional Coal Combustion Process," CHAM Company Report No. PDR/ CHAM UK/ 8, May 1982.
15. Svehla A. L., "Estimated Viscosities and Thermal Conductivities of Gases at High Temperatures," NASA TR R-132, 1962.
16. Prentice J. L., "Aluminum Droplet Combustion: Rates and Mechanisms in Wet and Dry Oxidizers," AD - 778 037, NWC, China Lake, CA., Apr. 1974.

DISTRIBUTION LIST

		No. Copies
1.	Defense Technical Information Center Cameron Station Alexandria, Virginia 22314	2
2.	Library, Code 0142 Naval Postgraduate School Monterey, California 93943-5100	2
3.	Department Chairman, Code 67 Department of Aeronautics Naval Postgraduate School Monterey, California 93943-5100	1
4.	Distinguished Professor Allen E. Fuhs Code 67Fu Naval Postgraduate School Monterey, California 93943-5100	2
5.	Mr. Donald E. Phillips, Code R10A White Oak Laboratory Naval Surface Weapons Center Silver Springs, Maryland 20910	3
6.	Dr. Franklin D. Hains, Code R14 White Oak Laboratory Naval Surface Weapons Center Silver Springs, Maryland 20910	1
7.	Mr. Wayne K. Reed, Code R14 White Oak Laboratory Naval Surface Weapons Center Silver Springs, Maryland 20910	1
8.	Information Services Division, Code X20 White Oak Laboratory Naval Surface Weapons Center Dahlgren, Virginia 22448	1
9.	Mr. George Daniello White Oak Laboratory Naval Surface Weapons Center Silver Springs, Maryland 20910	1
10.	Professor Oscar Biblarz Code 67Bi Department of Aeronautics Naval Postgraduate School Monterey, CA 93943-5100	1

11. Mr. Francis J. Romano, SEA 63R3 — 1
Naval Sea Systems Command
Washington, DC 20360

12. Dr. William Sykes, Code 175 — 1
David W. Taylor Naval Ship Research
and Development Center
Bethesda, Maryland 20084

13. Mr. Raymond P. Gogolewski — 1
Defense Advanced Research Project Agency
1400 Wilson Boulevard
Arlington, Virginia 22209

14. Mr. Charles Beatty — 1
Naval Undersea Center
San Diego, California 92132

15. Jonathan L. Minner — 1
Naval Surface Weapons Center
Dahlgren, Virginia 22448

16. Zernow Technical Services — 1
Attn: Louis Zernow
425 West Bonita
San Dimas, California 91773

17. Dr. Louis Baker, Jr. — 1
Argonne National Laboratories
9700 South Cass Avenue
Building 207
Argonne, Illinois 60439

18. R. G. S. Sewell — 1
Code 3835
Naval Weapons Center
China Lake, California 93555

19. Professor David Salinas — 1
Code 69Sa
Departwent of Mechanical Engineering
Naval Postgraduate Schhol
Monterey, CA 93943-5100

20. R. R. Durrell — 1
Code R12
Naval Surface Weapons Center
Silver Springs, Maryland 20910

21. D. R. Kennedy Associates, Inc. — 1
4940 El Camino Real, Suite 209
Post Office Box 4003
Mountain View, California 94040

22. Mr. J. M. McNerney — 1
Battelle
Columbus Laboratories
505 King Avenue
Columbus, Ohio 43201

23. Dr. G. E. Jensen — 1
Chemical Systems Division
United Technology Corporation
Post Office Box 358
Sunnyvale, California 94086

24. Dr. Edward G. Liszka — 1
Mark 50 Torpedo Office
Naval Sea Systems Command
Washington, DC 20360

25. Mr. Zeev Shavit (48) — 2
Ministry of Defense
P.O. Box 2250
Haifa, Israel

26. Professor A. Gany — 1
Department of Aeronautical Engineering
Technion - Israel Institute of Technology
Haifa, Israel

27. Research Administration — 1
Code 012A
Naval Postgraduate School
Monterey, CA 93943-5100